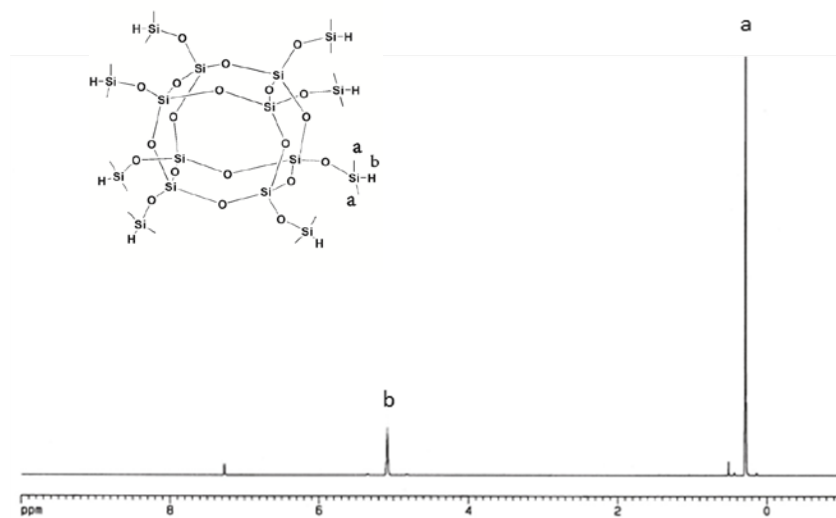
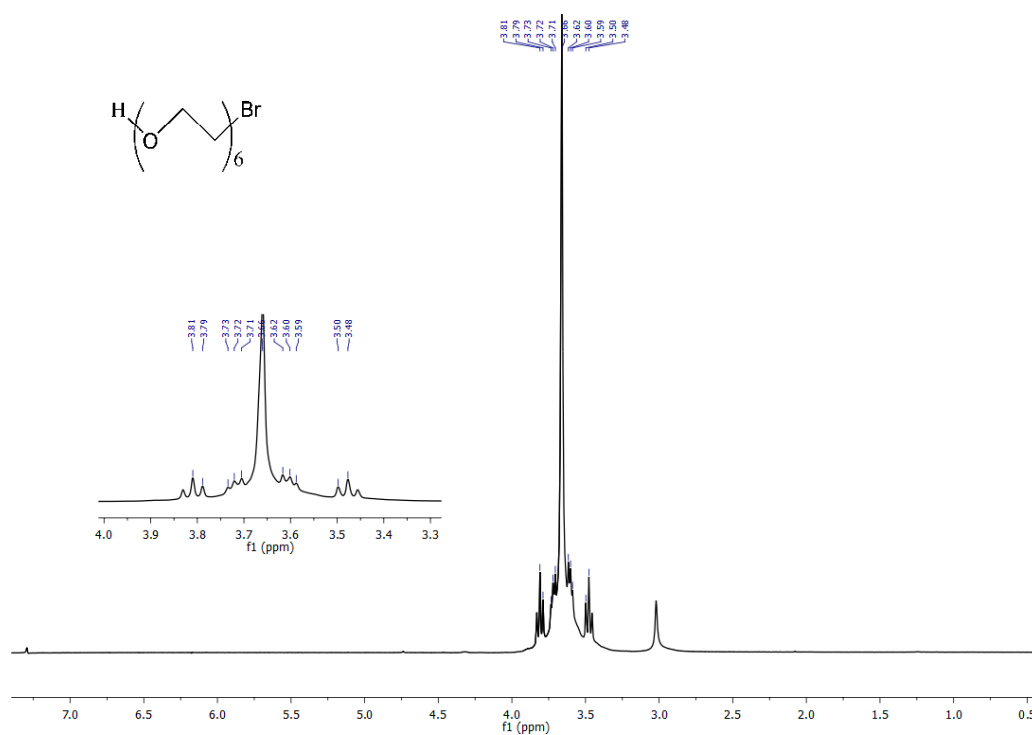


## Organic-Inorganic Hybrid Electrolytes from Ionic Liquid-Functionalized Octasilsesquioxane for Lithium Metal Batteries

Guang Yang, Chalathorn Chanthad, Hyukkeun Oh, Ismail Alperen Ayhan, and Qing Wang  
Department of Materials Science and Engineering, The Pennsylvania State University, University Park,  
Pennsylvania 16802, USA



**Figure S1.**  $^1\text{H}$  NMR spectrum of POSS.



**Figure S2.**  $^1\text{H}$  NMR spectrum of **2**.

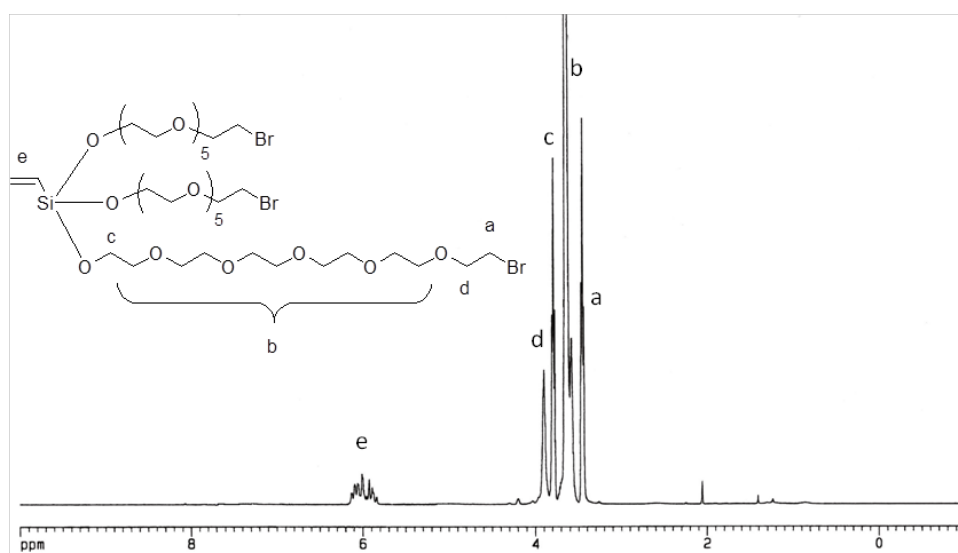


**Figure S3.**  $^1\text{H}$  NMR spectrum of **3**.

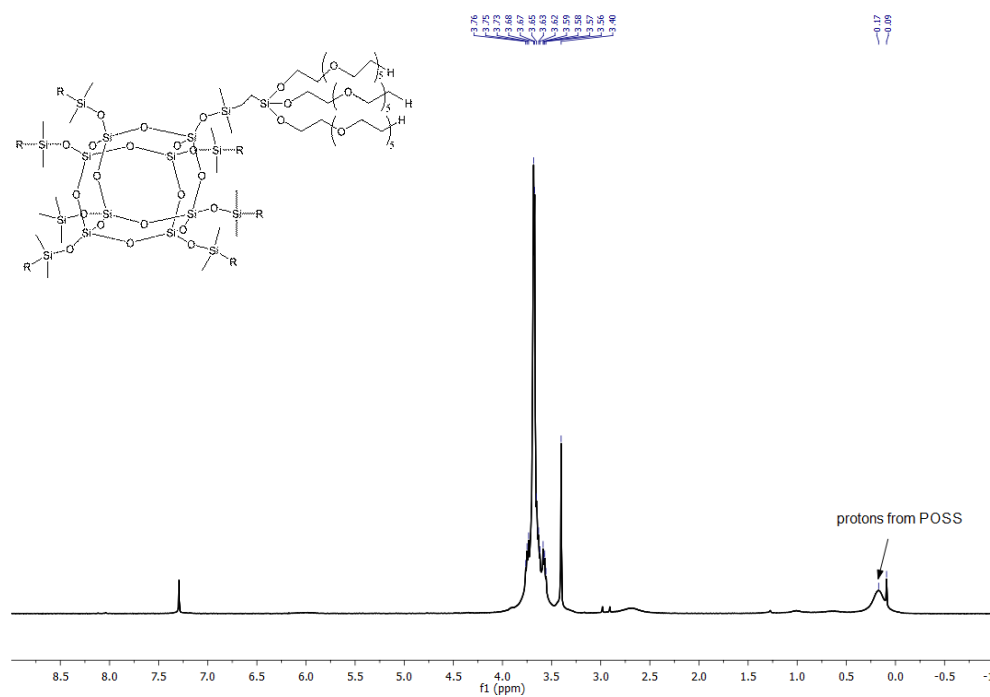


**Figure S4.**  $^1\text{H}$  NMR spectrum of POSS-PEO.  $^1\text{H}$  NMR (300 MHz,  $\text{CDCl}_3$ , ppm)  $\delta$ : 3.56-3.76 (m,  $-\text{O}-\text{CH}_2-$ ), 0.17 (s,  $\text{O}-\text{Si}(\text{CH}_3)_2-$ ).

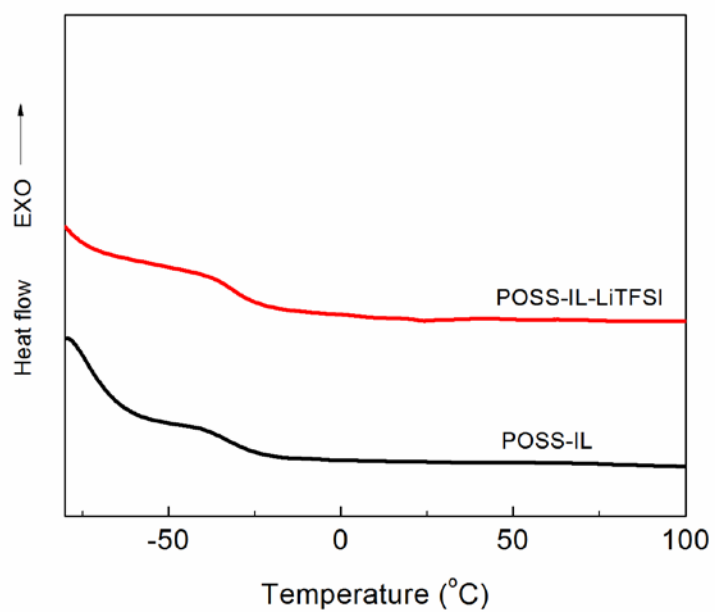


**Figure S5.** DSC curves of POSS-IL and POSS-IL-LiTFSI ([EO]/[Li]=12:1).

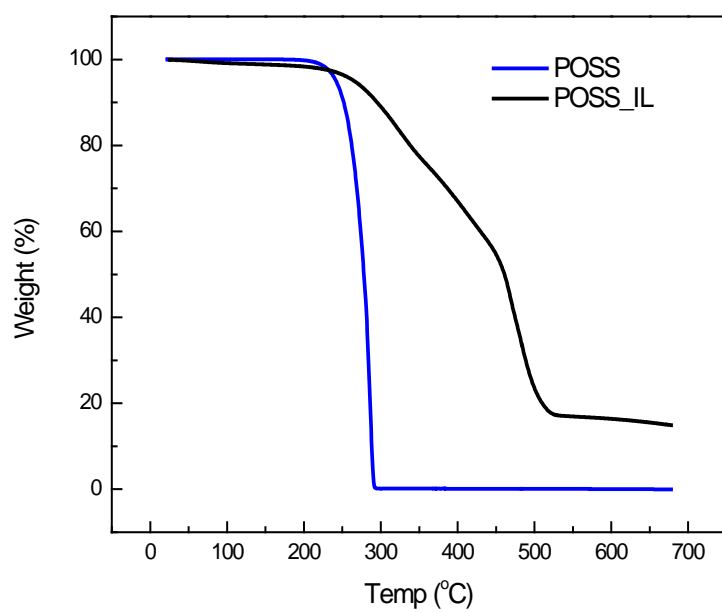


**Figure S6.** TGA curves of POSS-IL and POSS.

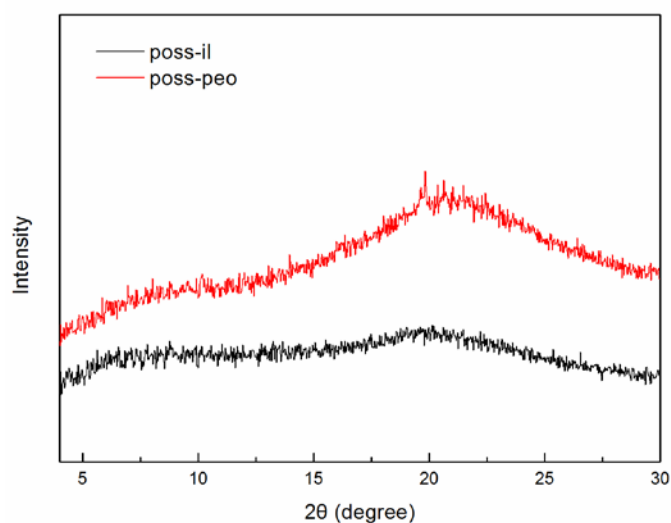


**Figure S7.** XRD patterns of POSS-IL and POSS-PEO.

The broad diffraction halo at  $2\theta=7^\circ$  (d-spacing of 1.25 nm) can be related to the POSS inter distance. Another diffraction halo at  $2\theta=20.1^\circ$  (d-spacing of 0.44 nm) could be assigned to the very weak signal of PEG in both POSS-IL and POSS-PEO, indicating the amorphous nature of the electrolytes.

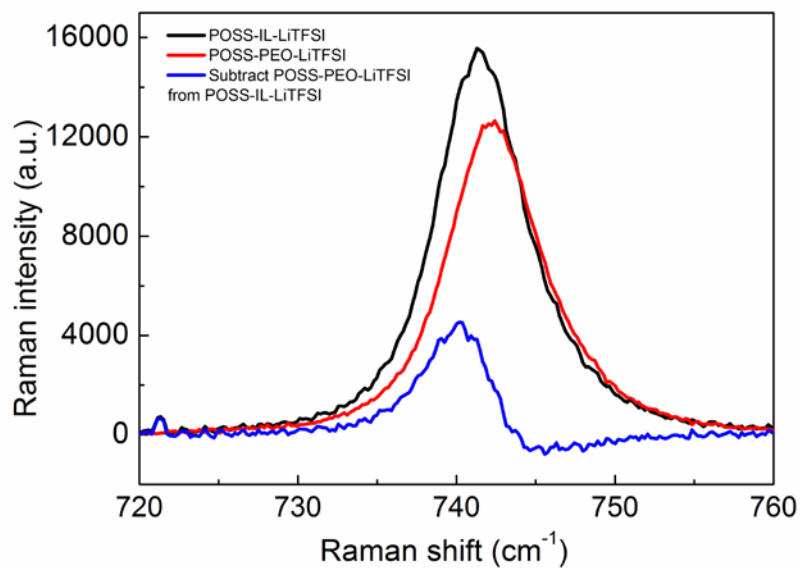


**Figure S8.** Raman spectra of TFSI- anion vibration of POSS-IL-LiTFSI (black), POSS-PEO-LiTFSI (red), and subtracting of POSS-PEO-LiTFSI from POSS-IL-LiTFSI (blue) at 25 °C in the range of 720-760  $\text{cm}^{-1}$ .

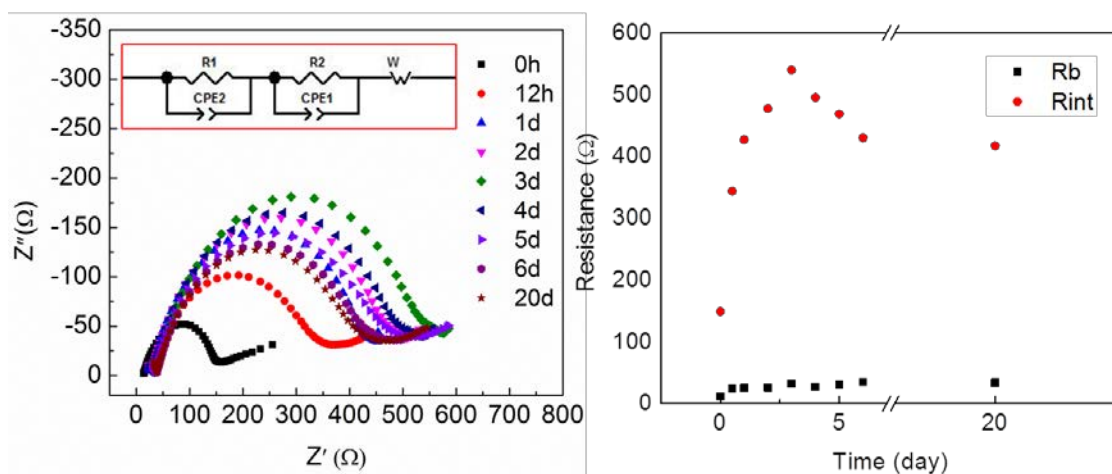


**Figure S9.** a) Nyquist plot of Li/POSS-IL-LiTFSI/Li symmetrical cell at different storage times. b) Evolution of  $R_{int}$  and  $R_b$  as a function of storage time. 25 °C.

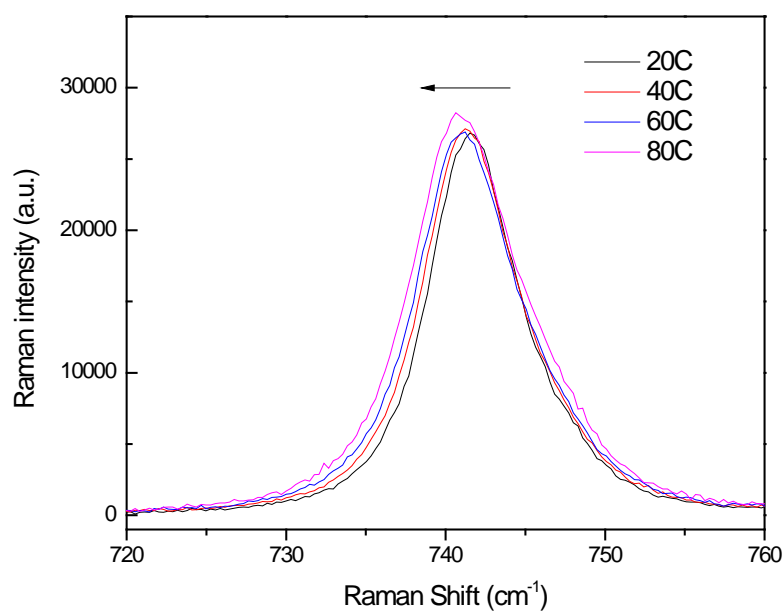


**Figure S10.** Temperature dependent Raman spectra in the TFSI<sup>-</sup> vibration region. Figure S1 showed the Raman bands of POSS-IL-LiTFSI around 742  $\text{cm}^{-1}$  at different temperatures. The band width increased and band position showed downshift when temperature was increased.

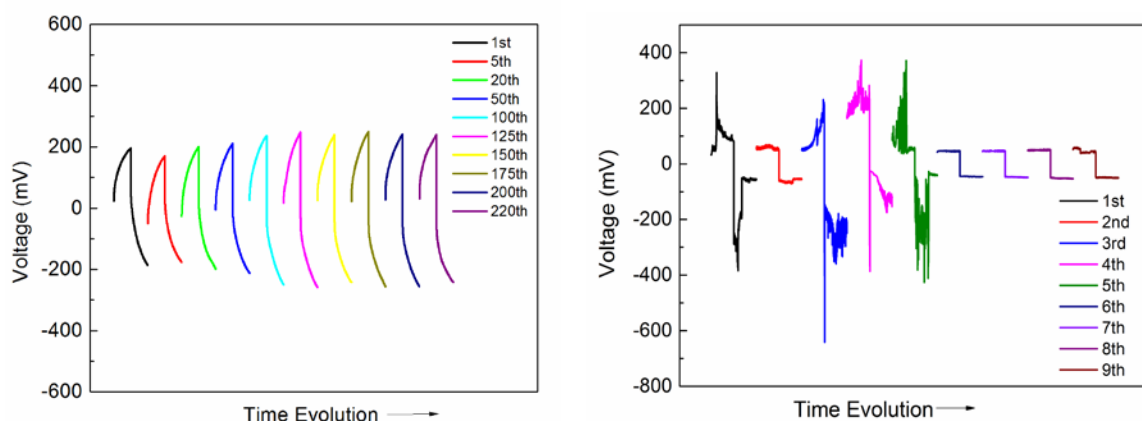


**Figure S11.** Selected galvanostatic stripping/plating cycles of Li/Li symmetrical cells with: left) POSS-IL-LiTFSI and right) 1 M LiTFSI in ED/DMC (1:1, v/v) at a current density of 0.05 mA/cm<sup>2</sup>. (each cycle includes 1 h stripping and 1 h plating)

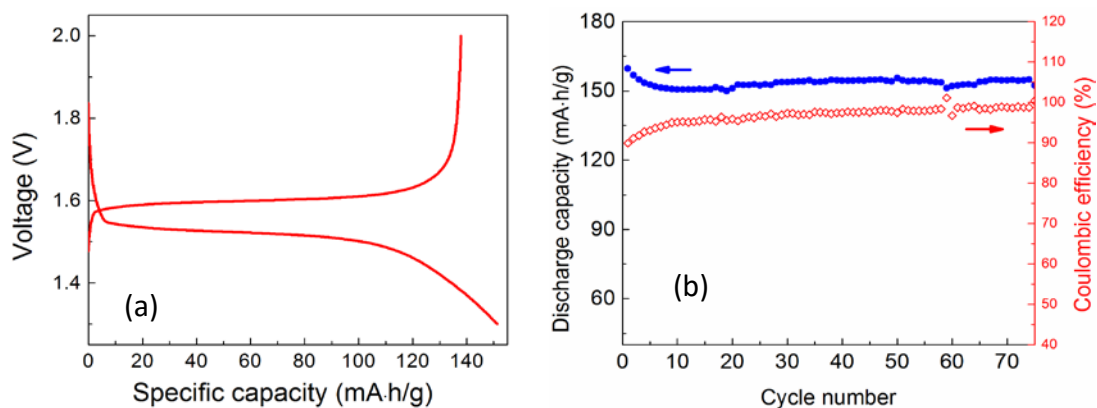


**Figure S12.** a) Typical voltage vs Specific Capacity profile of a galvanostatic charge-discharge cycling of Li/POSS-IL-LiTFSI/LTO cell at 0.1 C. b) Rate capability of Li/POSS-IL-LiTFSI/LTO cell. c) Cycling stability test of Li/POSS-IL-LiTFSI/LTO cell at 0.1 C. All tests were under 25 °C.

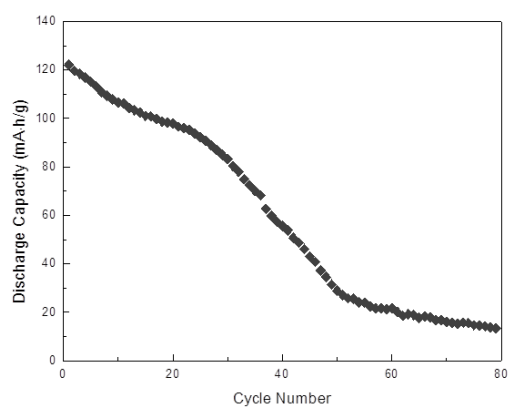


**Figure S13.** Cycling stability test of Li/POSS-PEO-LiTFSI/LFP at 60 °C and 0.1 C.

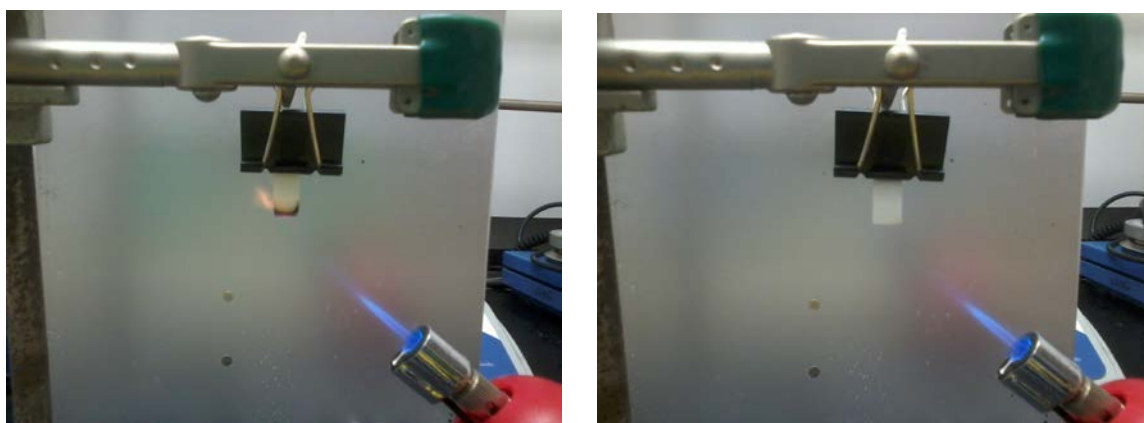


**Figure S14.** Flammability test of left) 1 M LiTFSI in EC/DMC. right) POSS-IL.